

THE QGP DISCOVERED AT RHIC

M. Gyulassy

Physics Department, Columbia University, New York, USA

gyulassy@nt3.phys.columbia.edu

Abstract Three empirical lines of evidence, (\mathbf{P}_{QCD} , \mathbf{p}_{QCD} , \mathbf{dA}), from RHIC have converged and point to the discovery of a strongly coupled Quark Gluon Plasma. The evidence includes (1) bulk collective elliptic flow and (2) jet quenching and mono-jet production, observed in Au+Au collisions at 200 AGeV, and (3) a critical control experiment using D+Au at 200 AGeV.

1. The Theoretical QGP

The Standard Model of strong interactions predicts the existence of a new phase of matter, called a Quark Gluon Plasma (QGP), in which the quark and gluon degrees of freedom normally confined within hadrons are mostly liberated. Lattice QCD calculations show that there is a rapid rise of the entropy density, $\sigma(T)$, of matter when the temperature reaches $T \approx T_c \sim 160$ MeV. Beyond T_c the effective number of degrees of freedom, $n(T)$, saturates near the number of quark and gluon helicity states $n_{\text{QCD}} = 8_c \times 2_s + \frac{7}{8} \times 3_c \times N_f \times 2_s \times 2_{q\bar{q}} \approx 37$. The entropy density $\sigma(T) = dP/dT = (\epsilon + P)/T \propto n(T)T^3$ approaches the Stefan Boltzmann limit $4P_{\text{SB}}(T)/3T$. The transition region is a smooth crossover when dynamical quarks are taken into account, but the width of the transition region remains relatively narrow, $\Delta T_c/T_c \sim 0.1$ [1]-[6].

The rapid rise of the entropy was predicted long before QCD by Hagedorn due to the observed exponential rise of the number of hadron resonances [5]. However, the saturation of the number of degrees of freedom near n_{QCD} is a unique feature of QCD. Even though the entropy density approaches the ideal, weakly interacting plasma limit, lattice calculations of correlators show that the QGP is far from ideal below $3T_c$. The nonideal nature of this strongly coupled QGP is also seen from the deviation of the pressure, $P(T)$, and energy density $\epsilon(T)$ from the Stefan Boltzmann limit as shown in Fig.(1) from [1].

The equation of state of the QGP, $P_{QCD}(T)$, is the bulk thermodynamic property that can be investigated experimentally via “barometric” observables. A measure of its stiffness is given by the speed of sound squared, $c_s^2 = dP/d\epsilon = d \log T/d \log \sigma = (3 + d \log n/d \log T)^{-1}$ shown in Fig.(2). Note that c_s^2 drops rapidly below 1/3 as the effective number of degrees of freedom drops when T approaches T_c . This softening of the QGP equation of state near T_c is a key feature can be looked for in the collective hydrodynamic flow patterns produced when the plasma expands.

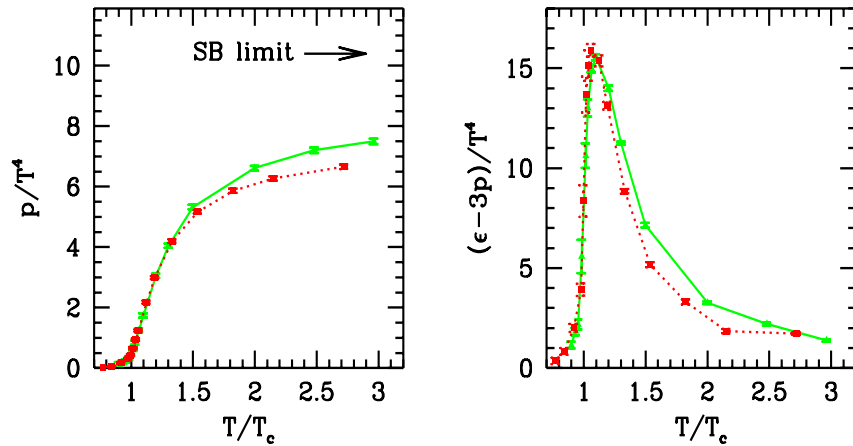


Figure 1. A recent Lattice QCD calculation [1] of the pressure, $P(T)/T^4$, and a measure of the deviation from the ideal Stefan-Boltzmann limit $(\epsilon(T) - 3P(T))/T^4$. Note that the scale on both graphs has not been corrected for finite lattice volume effects: see [2] for discussion.

Another distinctive feature of the QGP phase diagram is shown in the right panel in Fig.(2). Recent lattice QCD calculations [1] have begun to converge on numerical evidence that the QGP may have a second tricritical point [4, 6] at moderate baryon densities with $\mu_B = 3\mu_q \sim 360$ MeV and $T \sim T_c$.

QCD predictions of the QGP phase date back thirty years [7] and followed immediately after the discovery of asymptotic freedom of QCD. The experimental strategies to search for new forms of dense matter also date back thirty years when T.D. Lee proposed “vacuum engineering” [8]. It was then also realized by W. Greiner and collaborators [9–11] that extended regions of dense nuclear matter can be formed in high energy interactions of heavy nuclei, and that the measurement of collective flow patterns will provide the novel barometric probes of the equation of state of ultra-dense matter. The hunt for the QGP and other phases of nuclear matter has been underway since that time using several generations of higher energy accelerators, BEVALAC, AGS, SPS, and now RHIC, and covering an impressive energy range $\sqrt{s} - 2m_N = 0.2 - 200$ AGeV. In three years, LHC is expected to start vacuum engineering at 5500 AGeV.

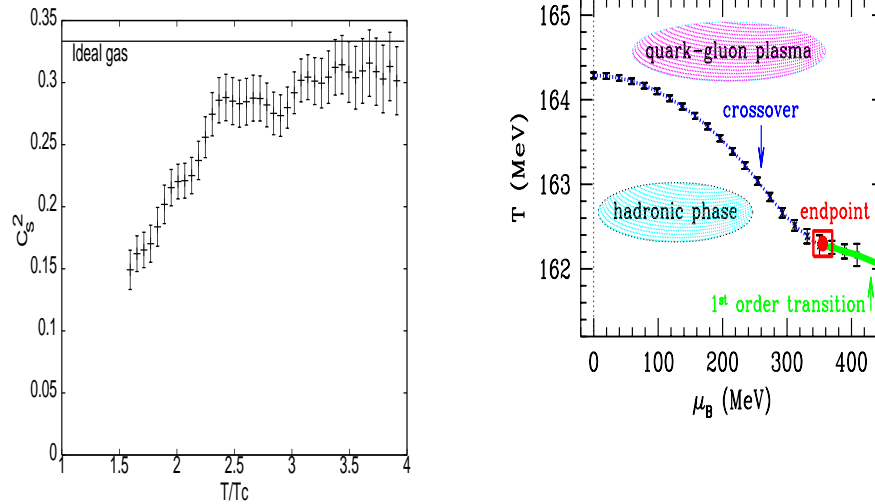


Figure 2. Important features of the QGP equation of state. The speed of sound [3] $c_s^2 = d\epsilon/dP$ drops below $1/3$ for $T < 2T_c \approx 300$ MeV. Right panel shows a current estimate of the location of the tricritical point at finite baryon density [1]

The first conclusive evidence for (highly dissipative) collective nuclear flow was seen at the BEVALAC in 1984 [12], and at AGS and SPS there after. However, the first conclusive evidence for nearly dissipation free collective flow obeying P_{QCD} had to await RHIC. In these lectures, the discovery of the novel low dissipation elliptic flow pattern at RHIC is highlighted as the first of three lines of evidence for QGP production at RHIC. Together with two other convergent lines of evidence, jet quenching and the critical $D + Au$ null control, I conclude that the QGP has not only been discovered but that a few of its remarkable properties have already been established experimentally.

2. The Empirical QGP

The discovery of the gedanken QGP phase of matter in the laboratory requires an empirical definition of the minimal number of necessary and sufficient conditions in terms of experimentally accessible observables. My empirical definition is summarized by the following symbolic equation

$$\text{QGP} = \mathbf{P}_{\text{QCD}} + \mathbf{p}_{\text{QCD}} + \mathbf{dA} \quad . \quad (1)$$

Why are three independent lines of evidence needed? The first term, \mathbf{P}_{QCD} , stands for a class of observables that provide information about its bulk thermo-

dynamic equation of state. The equation of state characterizes its *long wavelength* nonperturbative thermodynamic properties briefly reviewed in section 1.

The second term, **pQCD**, stands for class of observables that provide direct evidence about its *short wavelength* dynamics predicted by perturbative QCD. The QCD plasma differs qualitative from familiar abelian QED plasmas due to its unique non-Abelian color field dynamics. The radiative energy loss of energetic short wavelength partons was predicted to lead to striking quenching patterns [13]-[16] of moderate and high p_T hadrons. The high RHIC cm energy of 200 AGeV insures that $p_T \sim 10 - 20$ GeV jet production rates are large enough to measure via a wide array of inclusive and correlation observables. These hard partons serve as effective “external” tomographic probes of the the QGP and test its **pQCD chromo**-dynamics. Jets play the analogous role of neutrinos that probe the physics of stellar cores, while hadrons play the role of photons that probe the corona of the fireball.

Below RHIC energies, the **pQCD** line of evidence could not be fully developed because the jet rates decrease too rapidly with energy. However, even more importantly, at the lower $p_T < 4$ GeV available the effects of initial state nuclear dynamics and the final state hadronic dynamics could not be completely deconvoluted from the final spectra. This is the key point that I will repeatedly emphasize which differentiates the observables at the SPS and RHIC energies. The necessity to test for the same complications at RHIC is what gives rise to the third term in Eq.(1).

The third term, denoted by **dA**, stands for control experiments that can clearly differentiate between alternative nuclear dependences specific to *initial state* partonic wavefunctions as well as the production mechanisms. The control differential, **dA**, is critical at any energy because the QCD plasma must first be created from pure kinetic energy! There has been no hot QGP in the universe (except in cosmic ray collisions) since the last drop condensed into hadrons about 13 billion years ago. Cold crystalline quark matter may lurk in the cores of neutron stars, but the transient hot QGP must be “materialized” in the lab. The “matter” arises from decoherence of *virtual* quantum chromo fluctuations in the initial wavefunctions of high energy nuclei.

At ultra-relativistic energies, these virtual fluctuations are frozen out due to time dilation into what has been called a Color Glass Condensate (CGC) [17]. The CGC is the high density generalization of the Bjorken-Feynman dilute parton model. At high field strengths, the non-linear interactions of virtual quantum color fluctuations are predicted to limit the very small Bjorken $x_{BJ} \rightarrow 0$ Fourier components. The saturation property of CGC is related to unitarity constraints and determines the maximal entropy that can be produced in AA at a given \sqrt{s} as also pointed out by EKRT [18].

The **dA** control is needed to characterize to what extent these nonlinear initial state physics effects can be differentiated from effects due to final state

interactions in the QGP matter that forms from it. At RHIC, the best experimental handle on the dA term happens to be the study of $D + A$ reactions. In such light-heavy ion reactions, the initial state CGC physics can be isolated because the produced QGP, if any, is too tenuous.

Why don't I add more terms in Eq.(1)? In fact, each term stands for many independent components, as I elaborate below. For the three required terms in Eq.(1) the published experimental evidence is now overwhelming and conclusive. Four independent experiments have converged to complementary very high quality data sets.

The three terms in Eq.(1) are necessary and sufficient for establishing that a discovery has been made of a uniquely different form of strongly interacting QGP. After discussing the three lines of evidence, I will elaborate on why I believe that direct photons, J/ψ , HBT, or other interesting observables do not need to be added to Eq.(1). Those observable provide valuable additional constraints on the *combined and convoluted* properties of the initial state, the QGP, *AND* the dense hadronic matter into which it condenses. However, the deconvolution of the initial and hadronic final effects has already proven to be very difficult at SPS energies and will continue to be at RHIC.

To avoid misunderstanding, the discovery of the QGP does not mean that its physical properties are now understood. In fact, it only signals the beginning of a long and well focused direction of research. The history of the neutron star discovery offers an instructive analogy. In 1934 Baade and Zwicky proposed the theoretical existence of neutron stars soon after Chadwick discovered free neutrons. Thirty years later in 1967 Hewish and Bell observed the first few pulsars when suitable radio telescopes could finally be constructed. An amusing anecdote is that they actually agonized for a time about whether LGM (little green men) were sending them encrypted messages from the cosmos. T. Gold in 1968 (as $D + Au$ did at RHIC in 2003) put the debate to rest. Gold proposed that radiative energy loss of a magnetized neutron star would cause a predictable spin down. Later precision measurements confirmed this. Seventy years after its proposal, neutron star research still remains a very active experimental and theoretical direction of physics. Current interest has focused on possible *color field* super-conductivity [19] recently predicted in the very high μ_B sector of the QCD phase diagram, beyond the boundaries [6] of Fig.2b.

The critical $D + Au$ control experiments in 2003 could have found that the $Au + Au$ QGP observables were strongly distorted by the possible initial CGC state that created it. This would have certainly foiled Eq.(1). The search for the bulk QGP phase of matter would then have had to await higher energies and densities at LHC or for a better understanding of how to deconvolute that initial state physics. The large positive signatures in similar $p + Pb$ control experiments at SPS showed in fact initial effects strongly distort key observables. At SPS the physics of high p_T Cronin enhancement and $p + A \rightarrow J/\psi$

suppression remain the important open problems. In contrast, at RHIC energies, the absence of jet quenching at midrapidity and the “return of the jets” correlations in $d\mathbf{A} = \mathbf{D} + \mathbf{A}u$ provided the check-mate completion of Eq.(1).

As emphasized by McLerran[17] in these proceedings, the $D + Au$ control at RHIC at high rapidities does in fact produce a positive signature for new initial state physics. In those kinematic ranges $x_{BJ} < 0.001$, $d\mathbf{A}$ fails as a null control for QGP, but may signal the onset of nonlinear CGC initial conditions. In this lecture, I concentrate on the midrapidity region, $x_{BJ} > 0.01$, where Eq.(1) was conclusively satisfied.

3. P_{QCD} and Bulk Collective Flow

The identification of a new form of “bulk matter” requires the observation of novel and uniquely different collective properties from ones seen before. This requirement is the first term in Eq.(1). In heavy ion collisions, the primary observables of bulk collectivity are the radial, azimuthal and longitudinal flow patterns of hundreds or now thousands of produced hadrons. Stocker, Greiner, and collaborators were the first to predict [9–11, 20, 21] distinctive “side splash and squeeze-out” collective flow patterns in nuclear collisions. The different types of collective flows are conveniently quantified in terms of the first few azimuthal Fourier components [22], $v_n(y, p_T, N_p, h)$, of centrality selected triple differential inclusive distribution of hadrons, h . The centrality or impact parameter range is usually specified by a range of associated multiplicities, from which the average number of participating nucleons, N_p , can be deduced. The azimuthal angle of the hadrons are measured relative to a globally determined estimate for the collision reaction plane angle $\Phi(M)$. The “directed” v_1 and “elliptic” v_2 flow components [12, 22, 23]-[31] are readily identified from azimuthal dependence

$$\frac{dN_h(N_p)}{dydp_T^2d\phi} = \frac{dN_h(N_p)}{dydp_T^2} \frac{1}{2\pi} (1 + 2v_1(y, p_T, N_p, h) \cos \phi + 2v_2(y, p_T, N_p, h) \cos 2\phi + \dots) . \quad (2)$$

The “radial flow” component, “1”, is identified [32] from the hadron mass dependence of the blue shifted transverse momentum spectra

$$\frac{dN_h(N_p)}{dydp_T^2} \sim \exp[-m_h \cosh(\rho_\perp - \beta(y))/T_f] , \quad (3)$$

where $m_h(\sinh(\rho_\perp), \cosh(\rho_\perp)) = (p_\perp, \sqrt{m_h^2 + p_\perp^2})$ and $\beta(y)$ is the mean collective transverse flow rapidity at y .

Figure (3) shows the striking bulk collectivity elliptic flow signature of QGP formation at RHIC. Unlike at SPS and lower energies, the observed large elliptic deformation $((1 + 2v_2)/(1 - 2v_2) \sim 1.5)$ of the final transverse momentum

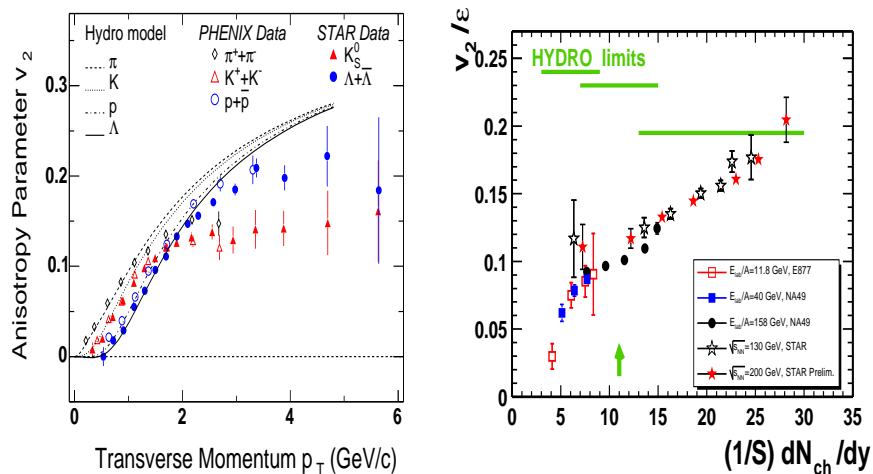


Figure 3. First line of evidence: Bulk collective flow is the barometric signature of QGP production. Left figure combines STAR [26]-[29] and PHENIX [30, 54] measurements of the azimuthal elliptic flow ($v_2(p_T)$) of π , K , p , Λ in Au+Au at 200 AGeV. The predicted hydrodynamic flow pattern from [33]-[37] agrees well with observations in the bulk $p_T < 1$ GeV domain. Right figure from [24] shows v_2 scaled to the initial elliptic spatial anisotropy, ϵ , as a function of the charge particle density per unit transverse area. The bulk hydrodynamic limit is only attained at RHIC.

distribution agrees for the first time with non-viscous hydrodynamic predictions [33]-[43] at least up to about $p_T \sim 1$ GeV/c. However, the right panel shows that when the local rapidity density per unit area [23, 24] drops below the values achieved at RHIC $\sim 30/\text{fm}^2$, then the elliptic flow (scaled by the initial spatial ellipticity, $\epsilon = \langle (y^2 - x^2)/(y^2 + x^2) \rangle$) falls below the perfect fluid hydrodynamic predictions. We will discuss in more detail the origin of the large discrepancy at SPS energies in the next section.

The most impressive feature in Fig.(3) is the agreement of the observed hadron mass dependence of the elliptic flow pattern for all hadron species, π , K , p , Λ , with the hydrodynamic predictions below 1 GeV/c. This is the QGP fingerprint that shows that there is a common bulk collective azimuthally asymmetric flow velocity field, $u^\mu(\tau, r, \phi)$.

The flow velocity and temperature fields of a perfect (non-viscous) fluid obeys the hydrodynamic equations:

$$\partial_\mu \{ [\epsilon_{QCD}(T(x)) + P_{QCD}(T(x))] u^\mu(x) u^\nu(x) - g^{\mu\nu} P_{QCD}(T(x)) \} = 0, \quad (4)$$

where $T(x)$ is the local temperature field, $P_{QCD}(T)$ is the QGP equation of state, and $\epsilon_{QCD}(T) = (T dP/dT - P)_{QCD}$ is the local proper energy density.

The above equations apply in the rapidity window $|y| < 1$, where the baryon chemical potential can be neglected. Eq.(4) provides the barometric connection between the observed flow velocity and the sought after P_{QCD} .

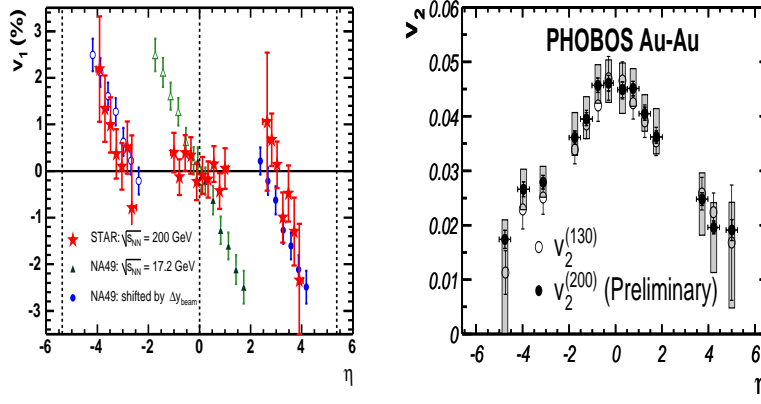


Figure 4. Left figure combines STAR and NA49 data [26] and shows that the directed side-wards flow, $v_1(y)$, is correlated over 8 units of rapidity at RHIC. At SPS collectivity is dominated by the overlapping fragmentation regions while at RHIC the nearly identical directed flow of in the fragmentation regions is shifted to $|y| > 2$. Right figure shows the pseudo rapidity dependence of elliptic from PHOBOS [31].

The long range nature of collective flow has also been conclusively established by STAR and PHOBOS seen in Fig.(4). The sideways flow is anti-correlated over 8 units of rapidity! In addition, its azimuthal orientation was shown to coincide with the azimuthal direction of the largest axis of elliptic deformation at $y = 0$. This provides an important test of the overall consistency of the hydrodynamic origin of flow. The rapidity dependence of the elliptic flow in Fig.(4) also shows the long range nature of bulk collectivity.

Why is v_2 more emphasized than v_1 or radial flow as a signature of QGP formation? The primary reason is that elliptic flow is generated mainly during the highest density phase of the evolution before the initial geometric spatial asymmetry of the plasma disappears. It comes from the azimuthal dependence of the pressure gradients, which can be studied by varying the centrality of the events [22]. Detailed parton transport [44] and hydrodynamic [39] calculations show that most of the v_2 at RHIC is produced before 3 fm/c and that elliptic flow is relatively insensitive to the late stage dissipative expansion of the hadronic phase. In contrast, radial flow has been observed at all energies [32] and has been shown to be very sensitive to late time ‘‘pion wind’’ radial pressure gradients [45], which continue to blow after the QGP condenses into hadronic resonances.

The observation of near ideal v_2 fluid collectivity as predicted with the P_{QCD} together with $v_1(y)$ and other consistency checks (c.c.) conclusively establish the first term in Eq.(1) :

$$\mathbf{P}_{QCD} = v_2(p_T; \pi, K, p, \Lambda) + v_1(y) + \text{c.c.} . \quad (5)$$

Preliminary Quark Matter 2004 analysis of Ξ, Ω flow are consistent with the predicted $v_2(p_T, y = 0, M, h)$ and this information is lumped into the c.c. terms in Eq.(5). Other data which provide consistency checks of the hydrodynamic explanation of collective flow include the observed π, K, p radial flow data [32] for $p_T < 2$ GeV. In addition, predicted statistical thermodynamic distributions [46] of final hadron yields agree remarkably well with RHIC data. Had hadro-chemistry failed at RHIC, then a large question mark would have remained about bulk equilibration in the QGP phase.

4. QGP Precursors at SPS and Dissipative Collectivity

It is important to point out, that no detailed 3+1D hydrodynamic calculation [41]-[43] has yet been able to reproduce the rapid decrease of $v_2(|\eta| > 1)$ observed by PHOBOS in Fig.(4). This discrepancy is due, in my opinion, to the onset of *hadronic* dissipation effects as the comoving density decreases with increasing y . From the right panel of Fig.(3), we see that as a decrease of the local transverse density from midrapidity RHIC conditions leads to an increasing deviation from the perfect fluid limit. The initial density was also observed to decrease at RHIC as $|y|$ increases [47]. Therefore, from SPS data alone, we should have expect deviations from the perfect fluid limit away from the midrapidity region. It would be interesting to superpose the PHOBOS data on top of the NA49 systematics.

To elaborate on this point, Fig.5 shows CERES data [48] on $v_2(p_T)$ at SPS energy $\sqrt{s} = 17$ AGeV. In agreement with the right panel of Fig.(3), the CERES data falls well below hydrodynamic predictions. At even lower energies, AGS and BEVALAC, the v_2 even becomes *negative* and this “squeeze out” of plane [11] is now well understood in terms of non-equilibrium BUU nuclear transport theory [25, 49]. In order to account for the smallness of v_2 at SPS, hydrodynamics has to be frozen out at unphysically high $T_f \approx T_c = 160$ MeV. However, the observed radial flow rules out this simple fix.

The discrepancy of v_2 and hydro at SPS energies can be traced to the important contribution of the dissipative final *hadronic* state interactions. The hadronic fluid is far from ideal. In approaches [45, 39] that combine perfect fluid QGP hydrodynamics with non-equilibrium hadronic transport dynamics, the importance of dissipative hadron dynamics at SPS was clearly demonstrated. The problem is that the QGP at lower initial densities condenses on a faster time scale cannot take advantage of the of the spatial asymmetry to generate large v_2 . The subsequent dissipative hadronic fluid is very inefficient

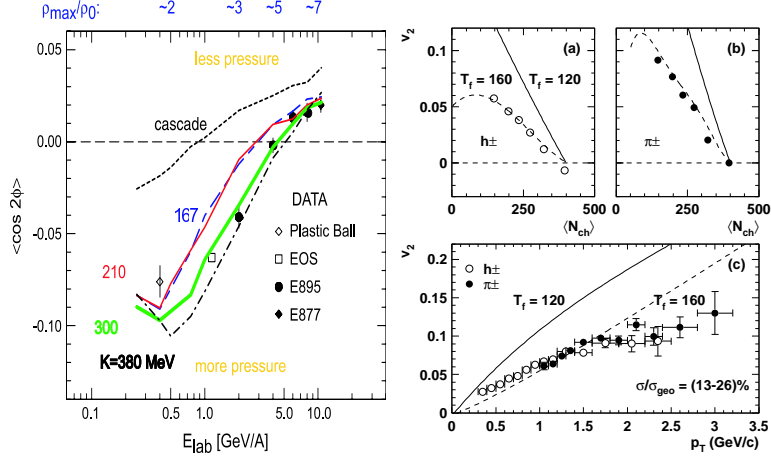


Figure 5. Evidence for dissipative collective flow below RHIC energies. Left: Non equilibrium BUU nuclear transport theory [49, 25] can explain the observed elliptic squeeze-out (negative v_2) collectivity below 4 AGeV. Right: CERES[48] data on elliptic flow at SPS is well below hydrodynamic predictions with freeze-out $T_f = 120$ MeV required to reproduce the single inclusive radial flow. Early freeze-out with $T_f = 160$ MeV, simulating effects of dissipation, is needed to reproduce the data.

in exploiting spatial asymmetry. A factor of two reduction of the initial QGP density, therefore, leads to a significant systematic bias of the v_2 barometer, not only at SPS but also at high $|y|$ at RHIC. Current hadronic transport theory is not yet accurate enough to re-calibrate the barometer away from mid-rapidities at RHIC.

In light of the above discussion, the smallness of dissipative corrections in the central regions of RHIC is even more surprising. At mid-rapidities, the lack of substantial dissipation in the QGP phase is in itself remarkable. Calculations based on parton transport theory [44] predict large deviations from the ideal non-viscous hydrodynamic limit. Instead, the data show that the QGP is almost a perfect fluid. A Navier Stokes analysis [40] is consistent with [44] and shows that the viscosity of the QGP must be about ten times less than expected if the QGP were a weakly interactive Debye screened plasma. This unexpected feature of the QGP must be due to nonperturbative and hence strong coupling physics that persists to at least $3T_c$.

4.1 The Minimal Viscosity of the QGP

One intriguing theoretical possibility being explored in the literature [50] is that the shear viscosity, η , in the strongly coupled QGP may saturate at a universal super-string bound, $\eta/\sigma = 1/4\pi$. This conjectured duality between string theory and QCD may help to explain also the $\sim 20\%$ deviation

of $P_{QCD}(T)$ from the ideal Stefan Boltzmann limit. The discovery of nearly perfect fluid flow of *long wavelength* modes with $p_T < 1$ GeV at RHIC is certain to fuel more interest in this direction.

I propose that a simpler physical explanation of the lower bound on viscosity follows from the uncertainty principle, as derived in Eq.(3.3) of Ref. [51]. Standard kinetic theory derivation of shear viscosity leads to $\eta = (\rho\langle p\rangle\lambda)/3$ where ρ is the proper density, $\langle p\rangle$ is the average total momentum, and λ is the momentum degradation transport mean free path. The uncertainty principle implies that quanta with average momentum components $\langle p\rangle$ cannot be localized to better than $\Delta x \sim 1/\langle p\rangle$. Therefore the momentum degradation mean free path cannot be defined more accurately than $\lambda > 1/\langle p\rangle$. For an ultra-relativistic system, the entropy density is $\sigma \approx 4\rho$, therefore

$$\frac{\eta}{\sigma} > \frac{1}{12} , \quad (6)$$

which is within 5% of the string theory bound. It is the consequence of the universality of the Heisenberg uncertainty principle. Surprisingly, the QGP found at RHIC saturates this uncertainty bound and the data clearly rule out the order of magnitude larger predictions based on pQCD [51]. See again [44]. The long wavelength modes in the QGP are as maximally coupled as $\hbar = 1$ allows.

It is “shear” good luck that the mid rapidity initial conditions at RHIC are dense enough to essentially eliminate the dilution of elliptic flow due to the imperfect hadron fluid formed after the spatial asymmetry vanishes. (Recall that $(\eta/\sigma)_H \sim (T_c/T)^{1/c_H^2} > 1$ for $T < T_c$ [51]). At lower energies or higher rapidities this good luck runs out and the mixture of near perfect QGP and imperfect hadronic fluid dynamics reduces the elliptic flow.

5. pQCD and Jet Quenching

In addition to the breakdown of perfect fluid collectivity at high rapidity seen in Fig.(4), Fig.(3) clearly shows that hydrodynamics also breaks down at very short wavelengths and high transverse momenta, $p_T > 2$ GeV. Instead of continuing to rise with p_T , the elliptic asymmetry stops growing and the difference between baryon vs meson v_2 reverses sign! Between $2 < p_T < 5$ GeV the baryon $v_2^B(p_T)$ exceeds the meson $v_2^M(p_T)$ by approximately 3/2. For such short wavelength components of the QGP, local equilibrium simply cannot be maintained due the fundamental asymptotic freedom property of QCD. I return to the baryon dominated transition region $1 < p_T < 5$ GeV in a later section since this involves interesting but as yet uncertain non-equilibrium non-perturbative processes. In this section I concentrate on the $p_T > 2$ GeV meson observables that can be readily understood in terms QGP modified pQCD dynamics [13, 14].

The quantitative study of short wavelength partonic **pQCD** dynamics focuses on the rare high p_T power law tails that extend far beyond the typical (long wavelength) scales $p < 3T \sim 1$ GeV of the bulk QGP. The second major discovery at RHIC is that the non-equilibrium power law high p_T jet distributions remain power law like but are strongly quenched [52]-[60]. Furthermore, the quenching pattern has a distinct centrality, p_T , azimuthal angle, and hadron flavor dependence that can be used to test the underlying dynamics in many independent ways. Below RHIC energies, the initial state Cronin enhancement

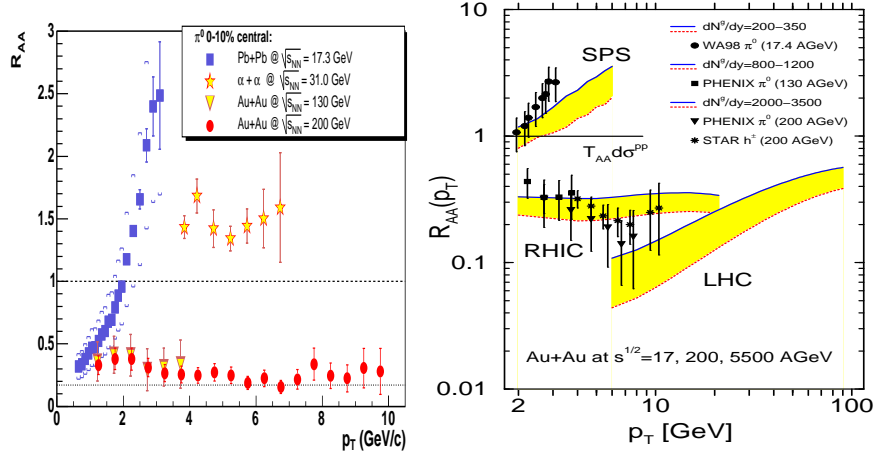


Figure 6. Jet Quenching at RHIC. Left [61] shows the jet quenching pattern of π^0 discovered by PHENIX [52, 53] at RHIC compared to previous observation of high p_T enhancement at ISR and SPS energies. The nuclear modification factor $R_{AA} = dN_{AA}/T_{AA}(b)d\sigma_{pp}$ measures the deviation of AA spectra from factorized pQCD. Right shows predictions [64] of the \sqrt{s} and p_T dependence from SPS, RHIC, LHC based on the GLV theory [65] of radiative energy loss.

of moderately high p_T tails was observed in central $Pb + Pb$ reactions at the SPS. At the ISR a reduced Cronin enhancement in $\alpha + \alpha$ reactions was seen. In contrast, at RHIC a large suppression, by a factor of 4-5, was discovered in central $Au + Au$ that extends beyond 10 GeV for π^0 .

Jet quenching in $A + A$ was proposed in [15, 16] as a way to study the dense matter produced at RHIC energies. As noted before, the pQCD jet production rates finally become large enough to measure yields up to high $p_T > 10$ GeV. Order of magnitude suppression effects were predicted based on simple estimates of induced gluon radiative energy loss. Ordinary, elastic energy loss [62] was known by that time to be too small to lead to significant attenuation.

As reviewed in [13, 14] refinements in the theory since then have opened the possibility of using the observed jet quenching pattern as a tomographic tool [63] to probe the parton densities in a QGP. The right panel shows a recent jet tomographic analysis [64] of the PHENIX π^0 data [52, 53] based on the

GLV opacity formalism [65]. Vitev and I concluded from Fig.6b that the initial gluon rapidity density required to account for the observed jet quenching pattern must be $dN_g/dy \sim 1000 \pm 200$.

This jet tomographic measure of the initial dN_g/dy is in remarkable agreement with three other independent sources: (1) the initial entropy deduced via the Bjorken formula from the measured multiplicity, (2) the initial condition of the QGP required in hydrodynamics to produce the observed elliptic flow, and (3) the estimate of the maximum gluon rapidity density bound from the CGC gluon saturated initial condition [18].

These four independent measures makes it possible to estimate the maximal initial energy density in central collisions

$$\epsilon_0 = \epsilon(\tau \sim 1/p_0) \approx \frac{p_0^2}{\pi R^2} \frac{dN_g}{dy} \approx 20 \frac{\text{GeV}}{\text{fm}^3} \sim 100 \times \epsilon_A \quad (7)$$

where $p_0 \approx Q_{sat} \approx 1.0 - 1.4$ GeV is the mean transverse momentum of the initial produced gluons from the incident saturated virtual nuclear CGC fields [17, 18]. This scale controls the formation time $\hbar/p_0 \approx 0.2$ fm/c of the initially out-of-equilibrium (mostly gluonic) QGP. The success of the hydrodynamics requires that local equilibrium be achieved on a fast proper time scale $\tau_{eq} \approx (1-3)/p_0 < 0.6$ fm/c. The temperature at that time is $T(\tau_{eq}) \approx (\epsilon_0/(1-3) \times 12)^{1/4} \approx 2T_c$.

In HIJING model[66], the mini-jet cutoff is $p_0 = 2 - 2.2$ GeV limits the number of mini-jets well below 1000. The inferred opacity of the QGP is much higher and consistent with the CGC and EKRT estimates.

5.1 $R_{AA}(p_T)$ and Single Jet Tomography

In order to illustrate the ideas behind jet tomography, I will simplify the discussion here to a schematic form. See [13] for details. The fractional radiative energy loss of a high energy parton in an expanding QGP is proportional to the position weighed line integral over color charge density $\rho(\vec{x}_\perp, \tau)$

$$\Delta E_{GLV}/E \approx C_2 \kappa(E) \int_0^{L(\phi)} d\tau \tau \rho(\vec{x}_\perp(\tau), \tau) \quad , \quad (8)$$

where C_2 is the color Casimir of the jet parton and $\kappa(E)$ is a slowly varying function of the jet energy [13]. The azimuthal angle sensitive escape time, $L(\phi)$, depends on the initial production point and direction of propagation relative to the elliptic flow axis of the QGP [67]. For a longitudinal expanding QGP, isentropic perfect fluid flow implies that $\tau \rho(\tau) \approx (1/A_\perp) dN_g/dy$ is fixed by the initial gluon rapidity density. In this case

$$\frac{\Delta E(\phi)}{E} \propto C_2 \frac{L(\phi)}{A_\perp} \frac{dN_g}{dy} \propto C_2 N_{part}^{2/3} \frac{L(\phi)}{\langle L \rangle} \quad . \quad (9)$$

Therefore, gluon jets are expected to lose about 9/4 more energy than quarks. In addition, since the produced gluon density scales as the number of wounded participating nucleons at a given impact parameter, (9) predicts a particular centrality and azimuthal dependence of the energy loss. Detailed numerical studies show that the actual GLV energy loss can account qualitatively for the saturation of $v_2(p_T > 2)$ [67], the unexpected p_T independence [64] of the quenching pattern, the centrality dependence [54] of the suppression factor [68, 69], and the rapidity dependence [74] of $R_{AA}(\eta, p_T)$ [42, 69] for pions and high $p_T > 6$ GeV inclusive charged hadrons at RHIC.

To further illustrate qualitatively how (9) influences the quench pattern, consider a simplified initial jet distribution rate, $d^2N/d^2p_0 = cp_0^{-n}$ where $n \sim 7$. In applications these are of course calculated numerically. After passing through the QGP, the final jet $p_T = p_f = p_0(1 - \epsilon)$. The average over fluctuations constrains $\langle \epsilon \rangle = \Delta E(\phi)/E$. The quenched jet distribution is $d^2N/d^2p_T = (d^2p_0/d^2p_f)d^2N/d^2p_0 \approx (1 - \epsilon(\phi))^{n-2} cp_f^{-n}$. The calculated hadron inclusive distribution is obtained by folding the quench jet distribution over the fragmentation function $D(z = p_h/p_f, Q^2 = p_f^2)$. However, in this illustrative example the fragmentation function dependence drops out, and the nuclear modification factor, $R_{AA}(p_h, \phi, N_{part}) = dN_h(\epsilon)/dN_h(0)$ reduces to

$$R_{AA} = \langle (1 - \epsilon(\phi))^{n-2} \rangle \approx \left\langle \left(1 - \epsilon_c \frac{L(\phi)}{\langle L \rangle} \left(\frac{N_{part}}{2A} \right)^{2/3} \right)^{n-2} \right\rangle \quad (10)$$

The average over ϵ takes into account fluctuations of the radiative energy loss. The resulting R_{AA} is independent of p_T in this approximation. This was also found in the detailed numerical work in [64]. In central collisions, $N_{part} \approx 2A$ and $L(\phi) \approx \langle L \rangle$, and the magnitude of quenching is fixed by $\epsilon_c \propto dN_g/dy$. The centrality and azimuthal dependence for non-central collisions follows without additional calculations.

5.2 I_{AA} and Di-Jet Tomography

Measurements of near side and away side azimuthal angle correlations of di-jet fragments provide the opportunity to probe the evolution of the QGP color charge density in even more detail. Fig.(7) show the discovery [57–59] of mono-jet production [15] in central collisions at RHIC. In peripheral collisions, the distribution $dN/d\Delta\phi$ of the azimuthal distribution of $p_T \sim 2$ GeV hadrons relative to a tagged $p_T \sim 4$ GeV leading jet fragment shows the same near side and away side back-to-back jetty correlations as measured in $p + p$. This is a direct proof that the kinematic range studied tests the physics of pQCD binary parton collision processes. For central collisions, on the other hand, away side jet correlations are almost completely suppressed.

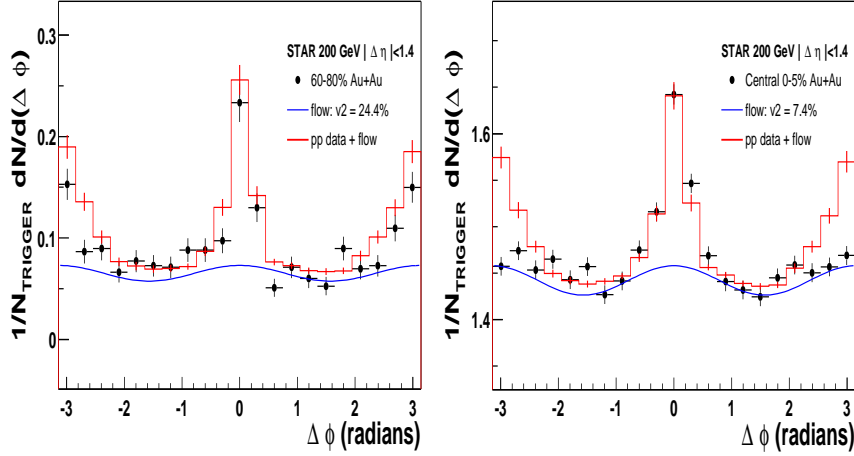


Figure 7. Monojets at RHIC from STAR [58, 59, 57]. Strongly correlated back-to-back di-jet production in pp and peripheral $AuAu$ left side is compared to mono-jet production discovered in central $AuAu$.

The quantitative measure of the nuclear modification of di-jet correlations in $A + B$ reactions at a given \sqrt{s} is given by a formidable multi-variable function

$$C_{AB}(y_1, p_{T1}, \phi_1, y_2, p_{T2}, \phi_2; b, \Phi_b, h_1, h_2) , \quad (11)$$

where (y_1, p_{T1}, ϕ_1) is the trigger particle of flavor h_1 and the (y_2, p_{T2}, ϕ_2) is an associated particle of flavor h_2 for collisions at an impact parameter b with a collective flow axis, the reaction plane, fixing the azimuthal angle Φ_b . Obviously C_{AB} is a very powerful microscope to study the modification of short wavelength correlations in the strongly interacting QGP.

The published data are as yet limited to $y_1 \approx y_2 \approx 0$, broad p_T cuts: $p_{T1} > 4$ GeV and $p_T \sim 2$ GeV, two bins of $\phi_1 - \phi_2$, and of course averaged over Φ_b . The measured modification of di-jet correlations is obtained by subtracting out the correlations due to bulk elliptic flow via the di-jet measure

$$I_{AA} = \int_{\Delta_-}^{\Delta_+} d(\phi_1 - \phi_2) \{ N(\phi_1 - \phi_2) - N_B(1 + 2v_2(p_1)v_2(p_2) \cos(2(\phi_1 - \phi_2))) \} , \quad (12)$$

where the number of triggered pairs $N(\phi_1 - \phi_2)$ is normalized relative to the expected number based on $p + p$ measurements in the same $[\Delta_-, \Delta_+]$ relative azimuthal angle range. Wang [70, 71] has analyzed the centrality, N_{part} , dependence of I_{AA} as well as R_{AA} and showed that both can be understood

from the same pQCD energy loss formalism. This provides another critical consistency check of jet tomography at RHIC.

Additional preliminary data from STAR presented by K. Filimonov at Quark Matter 2004 showed the first direct evidence that back-to-back dijet quenching has a distinctive dependence on the azimuthal orientation of the jets relative to the reaction plane as expected from the obvious generalization of Eq.(10)

$$I_{AA}(\Delta\phi = \pi, \Phi_b) \approx \langle \{ (1 - k_b L_1(\vec{r}_0, \hat{p}_T))(1 - k_b L_2(\vec{r}_0, -\hat{p}_T)) \}^{n-2} \rangle \quad (13)$$

where \vec{r}_0 is the initial transverse production point of the approximately back-to-back dijet moving in directions \hat{p}_T relative to the reaction plane Φ_b . Here k_b the effective fractional energy loss per unit length in the QGP produced at impact parameter b . The high p_{T1} trigger naturally biases \vec{r}_0 to be near the surface and \hat{p}_T is biased toward the outward normal direction. This means that on the average, $L_1 \ll L_2$, and the away side fragments should be strongly suppressed in the most central collisions, while the near side fragment correlations should be similar to that seen in pp . However, in non-central minimum biased events, Eq.(13) naturally predicts the away side fragments are less quenched when the trigger hadron lies in the reaction plane than perpendicular to it, as observed by STAR.

5.3 The Empirical pQCD Line of Evidence

Single and dijet data for pions above 3 GeV and protons above 6 GeV provide conclusive evidence that the QGP matter is partially opaque to short wavelength probes with a quenching pattern as predicted by the pQCD radiative energy loss:

$$\text{pQCD} = R_{AuAu}(p_T, \phi, N_{part}) + I_{AuAu}(\phi_1 - \phi_2; b, \Phi_b) . \quad (14)$$

With the vastly increased statistics from the current RHIC RUN 4, the tests of consistency of the theory will be further extended to $p_T \sim 20$ GeV, and I_{AA} and C_{AA} will attain ever greater resolving power. In addition, heavy quark tomography [76–78] will provide new tests of the theory.

6. The dAu Control

Only one year ago [79] the interpretation of high p_T suppression was under intense debate because it was not yet clear how much of the quenching was due to initial state saturation (shadowing) of the gluon distributions and how much due to jet quenching discussed in the previous section. There was only one way to find out - eliminate the QGP final state interactions by substituting a Deuterium beam for one of the two heavy nuclei. In fact, it was long ago anticipated [16] that such a control test would be needed to isolate the unknown nuclear gluon shadowing contribution to the A+A quench pattern. In addition

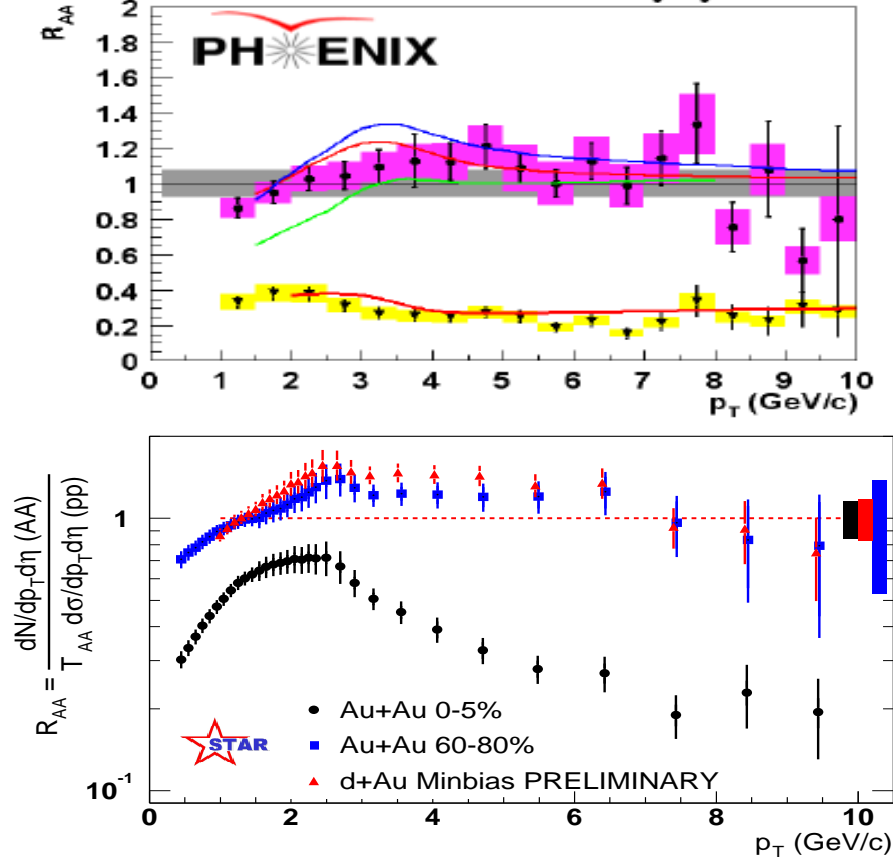


Figure 8. The **dA** control: PHENIX [72] π^0 and STAR [73] h^\pm data compare R_{DAu} to R_{AuAu} . These and BRAHMS [74] and PHOBOS [75] data prove that jet quenching in $Au+Au$ must be due to final state interactions. Curves for π^0 show predictions from [64] for $AuAu$ and from [82] DAu . The curves for DAu show the interplay between different gluon shadow parameterizations (EKS, none, HIJING) and Cronin enhancement and are similar to predictions in [80–82]. In lower panel, the unquenching of charged hadrons is also seen in $D + Au$ relative to $Au + Au$ at high p_T .

$D + Au$ was required to test predictions of possible initial state Cronin multiple interactions [80–82, 84]. In contrast, one model of CGC [83] predicted a 30% suppression in central $D+Au$.

The data [72–75] conclusively rule out large initial shadowing as the cause of the $x_{BJ} > 0.01$ quenching in $Au+Au$ and establish the empirical control analog of Eq.(14)

$$\mathbf{dA} = R_{DAu}(p_T, \phi, N_{part}) + I_{DAu}(\phi_1 - \phi_2, b) . \quad (15)$$

6.1 The “Return of the Jeti”

The I_{DAu} measurement from STAR [73] is the check mate! The return of

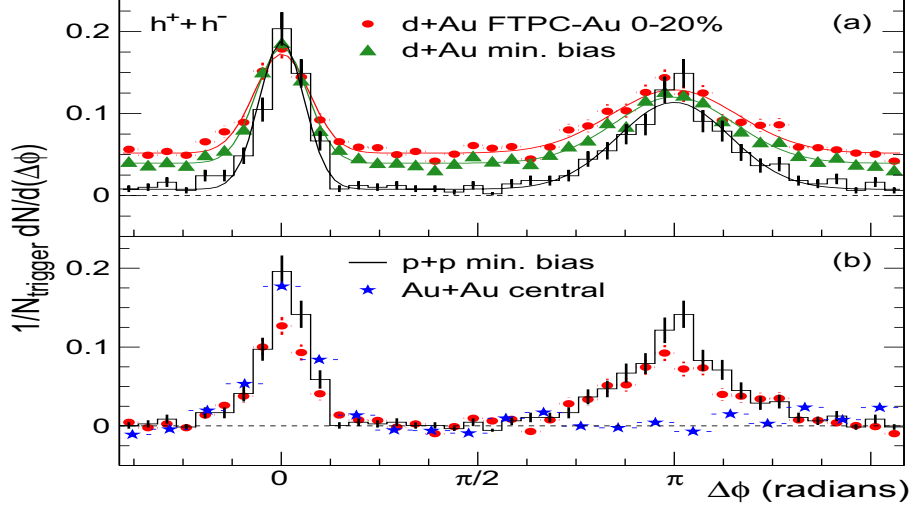


Figure 9. The **dA** “Return of the Jeti”: Dijet fragment azimuthal correlations from STAR [73] in DAu are unquenched relative to the mono jet correlation observed in central $AuAu$.

back-to-back jet correlation in $D + Au$ to the level observed in pp is seen in Fig.9. The data rule out CGC gluon fusion models that predict mono-jets [86] correlations in the $x_{BJ} > 0.01$ region. These $D + Au$ data support the conclusion [70, 71] that the observed jet quenching in $AuAu$ is due to parton energy loss.

Another independent check of the strikingly different nature of the nuclear matter created in $Au + Au$ versus $D + Au$ is provided by the width of the away side correlation function [87]. The transport properties of cold nuclear matter extracted from the Cronin enhancement effect [82] have only a small effect on the measured dijet acoplanarity. Preliminary PHENIX data presented by J. Rak at Quark Matter 2004 confirm the qualitative similarity of $p + p$ and $D + Au$ for $p_T > 2$ GeV, but at the same time demonstrate a strong quantifiable increase in acoplanarity in central $Au + Au$ consistent with multiple semi-hard scattering [88] in a dense QGP.

7. Conclusions

The three lines of evidence have converged from the four RHIC experiments. The empirical QGP that has been found at RHIC via the combination of Eqs.(1,5,14,15). This QGP is, however, not the weakly interacting [7], color-

dielectric “wQGP”, that we have searched for. Because of its near perfect fluid long wavelength properties, it must be very strongly coupled at least up to several times T_c . Symbolically, we should denote ¹ the empirical QGP at RHIC by “sQGP” to emphasize its special properties. The sQGP is not only a near perfect fluid but it also retains part of its QCD asymptotic freedom character through its highly suppressed, but power law, short wavelength spectrum.

In summary, the sQGP found RHIC was seen through the following three convergent lines of evidence

$$\begin{aligned}
\text{sQGP} &= \mathbf{P}_{\text{QCD}} + \mathbf{pQCD} + \mathbf{dA} \\
&= \{v_2(p_T; \pi, K, p, \Lambda) + v_1(y) + \text{c.c.}\} \\
&\quad + \{R_{AuAu}(p_T, \phi, N_{part}) + I_{AuAu}(\phi_1 - \phi_2; b, \Phi_b)\} \\
&\quad + \{R_{DAu}(p_T, \phi, N_{part}) + I_{DAu}(\phi_1 - \phi_2, b)\} . \quad (16)
\end{aligned}$$

Other surprising properties are already known. The anomalous $p_T = 2-5$ GeV baryon/meson ratios [27, 89], noted in connection with Fig.3 and also seen indirectly in Fig.8, already point to unexpected novel baryon number physics. Current speculations center around possible gluonic baryon junction dynamics [92], and possible multi-quark quark coalescence mechanisms [93]. The baryon number transport properties in the sQGP will certainly teach us new physics.

The experimental task of mapping out the novel properties of sQGP has only begun. It is important to concentrate, however, on those observables which are least distorted or “polluted” by uninteresting hadronic final interactions. For example, the severity of the HBT puzzle depends on which hadronic transport model is used. Pure hydrodynamics with late freeze-out times fails badly to reproduce final state soft pion correlations. Hybrid hydro+RQMD hadronic cascade does somewhat better [90], but there is at least one transport model [91] that reproduced the data. Non-equilibrium hadron resonance transport dynamics are unfortunately still not well enough understood at any energy to allow definitive conclusions to be drawn.

Thermal direct photons have yet to be measured, but it is already known that the pre-equilibrium [80] and hadronic final state contributions in the few GeV p_T range will produce large backgrounds on top of the thermal component. These must be deconvoluted if thermal photons are to serve as a sQGP thermometer. However, even the theoretical thermal photon rates are still under debate [94].

The J/ψ suppression discovery at SPS was originally attributed to Debye screening of $c\bar{c}$ in a wQGP paradigm. Recent lattice QCD results now indicate

¹I thank T.D.Lee for discussions and suggesting the sQGP designation of the matter discovered at RHIC to distinguish it from weakly interacting, Debye screened plasmas, wQGP, which may only exist at temperatures $T \gg T_c$.

that heavy quark correlations persist perhaps up to $2T_c$. This is another indication for the strongly coupled nature of **sQCD**. The suppression of J/ψ in AA is also strongly influenced by initial state and final state hadronic (comover) effects. It will be no easier to deconvolute these competing effects at RHIC. These observables of course need to be measured at RHIC, but one should not expect an easy interpretation.

I believe that the most promising direction of future experiments at RHIC will be precision measurements of short wavelength ($p_T > 2$ GeV) correlators C_{AB} illustrated in Eq.(11). These are very powerful six dimensional microscopes with four discrete (h_1, h_2, A, B) and two continuously adjustable geometric (b, Φ_b) experimental knobs in addition to the beam energy $\sqrt{s} = 20 - 200$ AGeV. One of the important correlators will be that of direct photon tagged jets [95]. Another will be open charm and possibly bottom quark tomographic probes. The available experimental knobs have hardly been varied yet. Much remains to be done to map out to clarify the properties of the **sQGP** found at RHIC.

Acknowledgments

This work was supported by the Director, Office of Energy Research, Office of High Energy and Nuclear Physics, Division of Nuclear Physics, of the U.S. Department of Energy under Contract DE-FG-02-93ER-40764. I also gratefully acknowledge partial support from an Alexander von Humboldt-Stiftung Foundation for continuation of collaborative work at the Institut für Theoretische Physik, Frankfurt.

References

- [1] Z. Fodor and S. D. Katz, arXiv:hep-lat/0402006. F. Csikor et al arXiv:hep-lat/0401022.
- [2] C. R. Allton et al, Phys. Rev. D **68**, 014507 (2003) [arXiv:hep-lat/0305007]. F. Karsch, E. Laermann and A. Peikert, Phys. Lett. B **478**, 447 (2000) [arXiv:hep-lat/0002003].
- [3] S. Gupta, Pramana **61**, 877 (2003) [arXiv:hep-ph/0303072].
- [4] M. A. Halasz et al, Phys. Rev. D **58**, 096007 (1998) [arXiv:hep-ph/9804290]. M. A. Stephanov, K. Rajagopal and E. V. Shuryak, Phys. Rev. Lett. **81**, 4816 (1998) [arXiv:hep-ph/9806219].
- [5] F. Karsch, K. Redlich and A. Tawfik, Phys. Lett. B **571**, 67 (2003) [arXiv:hep-ph/0306208].
- [6] D. H. Rischke, Prog. Part. Nucl. Phys. **52**, 197 (2004) [arXiv:nucl-th/0305030].
- [7] J. C. Collins and M. J. Perry, Phys. Rev. Lett. **34**, 1353 (1975); B. A. Freedman and L. D. McLerran, Phys. Rev. D **16**, 1169 (1977); G. Chapline and M. Nauenberg, Phys. Rev. D **16**, 450 (1977).
- [8] T. D. Lee and G. C. Wick, Phys. Rev. D **9**, 2291 (1974).
- [9] J. Hofmann, H. Stocker, W. Scheid and W. Greiner, On The Possibility Of Nuclear Shock Waves In Relativistic Heavy Ion Collisions, Bear Mountain Workshop, New York, Dec

1974. H. G. Baumgardt *et al.*, “Shock Waves And Mach Cones In Fast Nucleus-Nucleus Collisions,” *Z. Phys. A* **273**, 359 (1975).
- [10] H. Stocker, J. A. Maruhn and W. Greiner, *Z. Phys. A* **293**, 173 (1979). L. Csernai and H. Stocker, *Phys. Rev. C* **25**, 3208 (1981).
- [11] H. Stocker and W. Greiner, *Phys. Rept.* **137**, 277 (1986).
- [12] W. Reisdorf and H. G. Ritter, *Ann. Rev. Nucl. Part. Sci.* **47**, 663 (1997).
- [13] M. Gyulassy, I. Vitev, X. N. Wang and B. W. Zhang, arXiv:nucl-th/0302077. M. Gyulassy, *Lect. Notes Phys.* **583**, 37 (2002) [arXiv:nucl-th/0106072].
- [14] R. Baier, D. Schiff and B. G. Zakharov, *Ann. Rev. Nucl. Part. Sci.* **50**, 37 (2000) [arXiv:hep-ph/0002198].
- [15] M. Gyulassy and M. Plumer, *Nucl. Phys. A* **527**, 641 (1991). M. Gyulassy, M. Plumer, M. Thoma and X. N. Wang, *Nucl. Phys. A* **538**, 37C (1992)
- [16] X. Wang and M. Gyulassy, *Phys. Rev. Lett.* **68**, 1480 (1992).
- [17] L. McLerran, arXiv:hep-ph/0402137. E. Iancu and R. Venugopalan, arXiv:hep-ph/0303204. L. D. McLerran and R. Venugopalan, *Phys. Rev. D* **49**, 2233 (1994) [arXiv:hep-ph/9309289]. D. Kharzeev and E. Levin, *Phys. Lett. B* **523**, 79 (2001) [arXiv:nucl-th/0108006].
- [18] K. J. Eskola, K. Kajantie, P. V. Ruuskanen and K. Tuominen, *Phys. Lett. B* **543**, 208 (2002) [arXiv:hep-ph/0204034]; *Phys. Lett. B* **532**, 222 (2002) [arXiv:hep-ph/0201256].
- [19] M. G. Alford, J. Berges and K. Rajagopal, *Nucl. Phys. B* **571**, 269 (2000) [arXiv:hep-ph/9910254].
- [20] H. Stocker, J. A. Maruhn and W. Greiner, *Phys. Rev. Lett.* **44**, 725 (1980).
- [21] H. Stocker *et al.*, *Phys. Rev. C* **25**, 1873 (1982).
- [22] J. Y. Ollitrault, *Phys. Rev. D* **46**, 229 (1992).
- [23] S. A. Voloshin and A. M. Poskanzer, *Phys. Lett. B* **474**, 27 (2000) [arXiv:nucl-th/9906075].
- [24] C. Alt *et al.* [NA49 Collaboration], *Phys. Rev. C* **68**, 034903 (2003) [arXiv:nucl-ex/0303001].
- [25] G. Stoicea *et al.*, arXiv:nucl-ex/0401041.
- [26] J. Adams *et al.* [STAR Collaboration], arXiv:nucl-ex/0310029, *Phys. Rev. Lett.* **92** (2004) 062301.
- [27] P. R. Sorensen, hadronization of the bulk partonic matter created in Au + Au collisions at arXiv:nucl-ex/0309003. Ph.D. thesis.
- [28] J. Adams *et al.* [STAR Collaboration], arXiv:nucl-ex/0306007, *Phys. Rev. Lett.* **92** (2004) 052302
- [29] C. Adler *et al.* [STAR Collaboration], *Phys. Rev. C* **66**, 034904 (2002) [arXiv:nucl-ex/0206001].
- [30] S. S. Adler *et al.* [PHENIX Collaboration], *Phys. Rev. Lett.* **91**, 182301 (2003) [arXiv:nucl-ex/0305013].
- [31] B. B. Back *et al.* [PHOBOS collaboration], *Nucl. Phys. A* **715**, 65 (2003) [arXiv:nucl-ex/0212009].
- [32] Y. Cheng, F. Liu, Z. Liu, K. Schweda and N. Xu, *Phys. Rev. C* **68**, 034910 (2003). N. Xu *et al.* [NA44 Collaboration], *Nucl. Phys. A* **610**, 175C (1996).
- [33] P. F. Kolb, P. Huovinen, U. W. Heinz and H. Heiselberg, *Phys. Lett. B* **500**, 232 (2001).

- [34] P. Huovinen, P. F. Kolb, U. W. Heinz, P. V. Ruuskanen and S. A. Voloshin, Phys. Lett. B **503**, 58 (2001).
- [35] P. F. Kolb, U. W. Heinz, P. Huovinen, K. J. Eskola and K. Tuominen, Nucl. Phys. A **696**, 197 (2001).
- [36] P. Huovinen, arXiv:nucl-th/0305064.
- [37] P. F. Kolb and U. Heinz, arXiv:nucl-th/0305084.
- [38] D. Teaney, J. Lauret and E. V. Shuryak, nucl-th/0104041.
- [39] D. Teaney, J. Lauret and E. V. Shuryak, arXiv:nucl-th/0110037.
- [40] D. Teaney, Phys. Rev. C **68**, 034913 (2003). D. Teaney, arXiv:nucl-th/0301099.
- [41] T. Hirano and Y. Nara, Phys. Rev. Lett. **91**, 082301 (2003) [arXiv:nucl-th/0301042].
- [42] T. Hirano and Y. Nara, Phys. Rev. C **68**, 064902 (2003) [arXiv:nucl-th/0307087].
- [43] T. Hirano and Y. Nara, arXiv:nucl-th/0307015.
- [44] D. Molnar and M. Gyulassy, Nucl. Phys. A **697**, 495 (2002) [Erratum-ibid. A **703**, 893 (2002)] [arXiv:nucl-th/0104073]. B. Zhang, M. Gyulassy and C. M. Ko, Phys. Lett. B **455**, 45 (1999) [arXiv:nucl-th/9902016].
- [45] S. A. Bass and A. Dumitru, Phys. Rev. C **61**, 064909 (2000) [arXiv:nucl-th/0001033].
- [46] P. Braun-Munzinger, K. Redlich and J. Stachel, arXiv:nucl-th/0304013.
- [47] I. G. Bearden *et al.* [BRAHMS Collaboration], Phys. Rev. Lett. **88**, 202301 (2002) [arXiv:nucl-ex/0112001].
- [48] G. Agakichiev *et al.* [CERES/NA45 Collaboration], arXiv:nucl-ex/0303014.
- [49] P. Danielewicz, R. Lacey and W. G. Lynch, Science **298**, 1592 (2002) [arXiv:nucl-th/0208016].
- [50] G. Policastro, D. T. Son and A. O. Starinets, JHEP **0212**, 054 (2002) [arXiv:hep-th/0210220]. A. Buchel and J. T. Liu, arXiv:hep-th/0311175.
- [51] P. Danielewicz and M. Gyulassy, Phys. Rev. D **31** (1985) 53.
- [52] K. Adcox *et al.*, Phys. Rev. Lett. **88**, 022301 (2002); P. Levai *et al.*, Nucl. Phys. A **698**, 631 (2002).
- [53] K. Adcox *et al.* [PHENIX Collaboration], Phys. Lett. B **561**, 82 (2003) [arXiv:nucl-ex/0207009].
- [54] S. S. Adler *et al.* [PHENIX Collaboration], Phys. Rev. Lett. **91**, 072301 (2003) [arXiv:nucl-ex/0304022].
- [55] J. Adams *et al.* [STAR Collaboration], arXiv:nucl-ex/0305015.
- [56] C. Adler *et al.*, [STAR Collaboration] Phys. Rev. Lett. **89**, 202301 (2002) [arXiv:nucl-ex/0206011].
- [57] P. Jacobs and J. Klay [STAR Collaboration], arXiv:nucl-ex/0308023.
- [58] C. Adler *et al.* [STAR Collaboration], Phys. Rev. Lett. **90**, 082302 (2003) [arXiv:nucl-ex/0210033].
- [59] D. Hardtke [The STAR Collaboration], Nucl. Phys. A **715**, 272 (2003) [arXiv:nucl-ex/0212004].
- [60] C. Adler *et al.* [STAR Collaboration], Phys. Rev. Lett. **90**, 032301 (2003).
- [61] D. d'Enterria [PHENIX Collaboration], arXiv:nucl-ex/0401001.

- [62] J. D. Bjorken, FERMILAB-PUB-82-059-THY and erratum (unpublished); M. H. Thoma and M. Gyulassy, Nucl. Phys. B **351**, 491 (1991); E. Braaten and M. H. Thoma, Phys. Rev. D **44**, 2625 (1991); M. H. Thoma, J. Phys. G **26**, 1507 (2000) [arXiv:hep-ph/0003016].
- [63] M. Gyulassy, P. Levai, and I. Vitev, Phys. Lett. B **538**, 282 (2002); E. Wang and X.-N. Wang, Phys. Rev. Lett. **89**, 162301 (2002); C. A. Salgado and U. A. Wiedemann, Phys. Rev. Lett. **89**, 092303 (2002);
- [64] I. Vitev and M. Gyulassy, Phys. Rev. Lett. **89**, 252301 (2002) [arXiv:hep-ph/0209161].
- [65] M. Gyulassy, P. Levai and I. Vitev, Nucl. Phys. B **594**, 371 (2001) [arXiv:nucl-th/0006010]. Phys. Rev. Lett. **85**, 5535 (2000) [arXiv:nucl-th/0005032]; Nucl. Phys. B **571**, 197 (2000) [arXiv:hep-ph/9907461].
- [66] V. Topor Pop *et al.*, Phys. Rev. C **68**, 054902 (2003) [arXiv:nucl-th/0209089]. X. N. Wang and M. Gyulassy, Phys. Rev. D **44**, 3501 (1991).
- [67] M. Gyulassy, I. Vitev and X. N. Wang, Phys. Rev. Lett. **86**, 2537 (2001) [arXiv:nucl-th/0012092]. M. Gyulassy, I. Vitev, X. N. Wang and P. Huovinen, Phys. Lett. B **526**, 301 (2002) [arXiv:nucl-th/0109063].
- [68] M. Gyulassy, CIPANP Conference seminar, May 21, 2003, "<http://www.phenix.bnl.gov/WWW/publish/nagle/CIPANP/>"
- [69] A. Adil, M. Gyulassy, I. Vitev, to be published.
- [70] X. N. Wang, arXiv:nucl-th/0305010.
- [71] X. N. Wang, Phys. Lett. B **579**, 299 (2004) [arXiv:nucl-th/0307036].
- [72] S. S. Adler *et al.* [PHENIX Collaboration], Phys. Rev. Lett. **91**, 072303 (2003) [arXiv:nucl-ex/0306021].
- [73] J. Adams *et al.* [STAR Collaboration], Phys. Rev. Lett. **91**, 072304 (2003) [arXiv:nucl-ex/0306024].
- [74] I. Arsene *et al.* [BRAHMS Collaboration], suppression," Phys. Rev. Lett. **91**, 072305 (2003) [arXiv:nucl-ex/0307003].
- [75] B. B. Back *et al.* [PHOBOS Collaboration], Phys. Rev. Lett. **91**, 072302 (2003) [arXiv:nucl-ex/0306025].
- [76] Y. L. Dokshitzer and D. E. Kharzeev, Phys. Lett. B **519**, 199 (2001) [arXiv:hep-ph/0106202].
- [77] M. Djordjevic and M. Gyulassy, Nucl. Phys. A **733**, 265 (2004) [arXiv:nucl-th/0310076].
- [78] S. Batsouli, S. Kelly, M. Gyulassy and J. L. Nagle, Phys. Lett. B **557**, 26 (2003) [arXiv:nucl-th/0212068].
- [79] Transverse Dynamics at RHIC, BNL March 6-8, 2003, "http://www.phenix.bnl.gov/phenix/WWW/publish/rak/workshop/int/program_TD.htm"
- [80] X. N. Wang, Phys. Rev. C **61**, 064910 (2000) [arXiv:nucl-th/9812021].
- [81] X. N. Wang, Phys. Rept. **280**, 287 (1997) [arXiv:hep-ph/9605214].
- [82] I. Vitev, Phys. Lett. B **562**, 36 (2003) [arXiv:nucl-th/0302002]; A. Accardi and M. Gyulassy, arXiv:nucl-th/0308029; P. Levai, G. Papp, G. G. Barnafoldi and G. I. Fai, arXiv:nucl-th/0306019.
- [83] D. Kharzeev, E. Levin and L. McLerran, Phys. Lett. B **561**, 93 (2003) [arXiv:hep-ph/0210332].
- [84] J. w. Qiu and I. Vitev, arXiv:hep-ph/0309094; arXiv:hep-ph/0401062.
- [85] S. A. Bass *et al.*, Prog. Part. Nucl. Phys. **41**, 225 (1998) [arXiv:nucl-th/9803035].

- [86] V. R. Zoller, arXiv:hep-ph/0306038.
- [87] J. w. Qiu and I. Vitev, Phys. Lett. B **570**, 161 (2003) [arXiv:nucl-th/0306039]; I. Vitev, arXiv:nucl-th/0308028.
- [88] M. Gyulassy, P. Levai and I. Vitev, Phys. Rev. D **66**, 014005 (2002) [arXiv:nucl-th/0201078].
- [89] S. S. Adler *et al.* [PHENIX Collaboration], arXiv:nucl-ex/0307022.
- [90] S. Soff, S. A. Bass and A. Dumitru, Phys. Rev. Lett. **86**, 3981 (2001) [arXiv:nucl-th/0012085].
- [91] Z. w. Lin, C. M. Ko and S. Pal, Phys. Rev. Lett. **89**, 152301 (2002) [arXiv:nucl-th/0204054].
- [92] D. Kharzeev, Phys. Lett. B **378**, 238 (1996) [arXiv:nucl-th/9602027]. S. E. Vance et al, Phys. Lett. B **443**, 45 (1998) [arXiv:nucl-th/9806008]. I. Vitev and M. Gyulassy, Phys. Rev. C **65**, 041902 (2002) [arXiv:nucl-th/0104066].
- [93] P. Csizmadia, et al J. Phys. G **25**, 321 (1999) [arXiv:hep-ph/9809456]. R. J. Fries, B. Muller, C. Nonaka and S. A. Bass, Phys. Rev. Lett. **90**, 202303 (2003) [arXiv:nucl-th/0301087]. D. Molnar and S. A. Voloshin, Phys. Rev. Lett. **91**, 092301 (2003) [arXiv:nucl-th/0302014]. V. Greco, C. M. Ko and P. Levai, Phys. Rev. C **68**, 034904 (2003) [arXiv:nucl-th/0305024]. Z. W. Lin and D. Molnar, Phys. Rev. C **68**, 044901 (2003) [arXiv:nucl-th/0304045].
- [94] F. Gelis, Nucl. Phys. A **715**, 329 (2003) [arXiv:hep-ph/0209072].
- [95] X. N. Wang, Z. Huang and I. Sarcevic, Phys. Rev. Lett. **77**, 231 (1996) [arXiv:hep-ph/9605213].